DOI: https://doi.org/10.15276/ict.03.2026.38
UDC 681.5:004.89

Dynamic adaptation of chaotic motion parameters of unmanned aerial vehicles based on terrain complexity analysis

Mykyta S. Kozlov[1)]
ORCID: https://orcid.org/0009-0007-0071-7748; nikita.kozlov@stud.onu.edu.ua
Eugene V. Malakhov[1)]
ORCID: https://orcid.org/0000-0002-9314-6062; eugene.malakhov@onu.edu.ua. Scopus Author ID: 56905389000
[1)] Odesa I. I. Mechnikov National University, 2, Dvoryanskaya Str. Odesa, 65082, Ukraine

ABSTRACT

Autonomous unmanned aerial vehicle swarms are increasingly deployed in emergency response and search-and-rescue operations. Existing waypoint-based trajectory planners, however, leave systematic coverage gaps in non-convex areas and cannot adapt once conditions change mid-mission. This paper proposes a terrain-aware adaptive chaotic motion algorithm that tunes swarm motion parameters online from measurable geometric properties of the operational area, including the concavity index, obstacle density, narrow corridor coefficient and real-time coverage progress indicators. A closed-loop adaptive controller matches the terrain profile with nine swarm parameters using a linear interpolation-based rule with smoothing. Experimental evaluation based on fifty simulation tests shows that adaptive mode provides fifteen percents higher average area coverage, reducing the spread between runs by nineteen percents, compared to the baseline variant with fixed parameters. Statistical analysis using the Mann–Whitney U test confirms that improvements in regional-level coverage in terms of total distance and energy consumption are highly significant, whereas differences in redundant scanning and obstacle density are not. These results emphasise that the main operational advantages of the adaptive algorithm are reliable and reproducible, while secondary indicators remain stable in all modes. The results confirm that chaotic adaptation with consideration of terrain relief is a fundamental and operationally viable strategy for autonomous territory scanning.

Keywords: Information technology; swarm intelligence; chaotic algorithm; multi-agent systems; scan optimization; swarm trajectory optimization; scanning area analysis

For citation: **Kozlov M. S., Malakhov E. V. "Dynamic adaptation of chaotic motion parameters of unmanned aerial vehicles based on terrain complexity analysis".** ***Informatics. Culture. Technology*****. 2026; Vol. 3 No. 1(3): 493–504. DOI: https://doi.org/10.15276/ict.03.2026.38**

The study aims to develop an adaptive chaotic motion algorithm for Unmanned Aerial Vehicle (UAV) swarms that takes the terrain's characteristics into account and dynamically adjusts motion parameters based on the operational area's measurable geometric properties, and to establish statistically whether such a closed-loop mapping produces superior coverage outcomes compared with a static optimally-tuned parameter set.

Introduction. Emergency response operations require autonomous systems capable of rapidly scanning complex geographic areas. Unmanned Aerial Vehicle swarms provide superior coverage and fault tolerance compared to single-agent systems, but from an algorithmic perspective, achieving complete coverage of an area in a short time frame remains a challenging task. Mountain rescue scenarios illustrate this relevance, for example, the chances of survival for avalanche victims decrease sharply over time [1]. Route planning for solar-powered UAVs in mountain search and rescue operations [2] demonstrates that trajectory design considering energy consumption is as important as coverage quality, especially for long-duration operations in challenging terrain. Existing waypoint-based algorithms generate predictable patterns with systematic gaps in coverage in irregular terrain and lack flexibility when environmental conditions change, which is a critical limitation in emergency situations.

Unmanned Aerial Vehicle swarm technology has matured significantly in the areas of communication architectures [3], control systems [4], and swarm-level stability analysis [5], [6]. However, despite this progress, the coordination of large heterogeneous swarms in real time in non-convex territories remains an unsolved problem. Network vulnerability studies [7] confirm that swarm connectivity deteriorates nonlinearly as agents are lost or isolated, making adaptive coordination a prerequisite for mission-critical operations.

The multi-level architecture for scanning disaster areas proposed by Tsaryuk and Malakhov [8] demonstrated that distributed swarm intelligence can coordinate scanning missions without central control, but the underlying motion strategy remained deterministic. Furthermore, heterogeneous swarms with different battery characteristics and sensor capabilities require algorithms that balance coverage efficiency and energy constraints [9].

The issue of survivability of reconnaissance swarms when agents are lost is addressed by Sambursky and Malakhov [10] through reconfiguration based on cellular automata, which defines fault tolerance as a key requirement for the configuration of operational UAV swarms. In parallel, Kozlov and Shvets [11] demonstrate that the principles of "swarm chemistry" allow for complex multi-level reconfiguration of heterogeneous swarms, creating a theoretical framework that is expanded upon in this work. The practical application of multi-level drone systems in emergency human recognition tasks [12] further motivates the need for effective territory coverage as a prerequisite for the effective execution of higher-level missions.

This article applies deterministic chaos theory to UAV swarm coordination. The ergodic properties of chaotic motion models produce efficient exploratory behavior; combined with the principles of "swarm chemistry" (separation, cohesion, and alignment, anti-jamming), they yield emergent coordination that systematically improves coverage while preserving collision avoidance and energy efficiency.

Related work. Research on multi-UAV coordination falls into three algorithmic paradigms, each with strengths and limitations that bear directly on the present work.

Deterministic path planning with dynamic adaptation. Liu et al. [13] propose an improved $A*$ algorithm that adds artificial potential field repulsion terms and time-evolving dynamic risk modeling. Heuristic weights are adjusted from spatiotemporal collision risk, which performs well when obstacles are in motion. The $O(n^2)$ cost of pairwise threat assessment and the reliance on known obstacle trajectories, however, limit its use in uncertain, rapidly evolving environments.

Artificial potential field methods and hybrid approaches. Hu et al. [14] develop a hybrid Multi-Robot Formation APF approach with auxiliary sub-goal generation, reducing heading angle changes by 84% compared with traditional APF. Despite this improvement, the algorithm exhibits declining gains with increasing swarm size (path reduction drops from 6.6% to 2.3% in 5-UAV scenarios), suggesting scalability limitations in large heterogeneous deployments.

Physics-based swarm coordination. Keribayeva et al. [15] model swarm obstacle avoidance through Newton's second law discretization, demonstrating topology transformations (cubic, circular, hierarchical) during mission execution. While the physical grounding provides interpretable motion equations, the Courant stability constraint ($C \leq 0.5$) substantially increases computational overhead and restricts the approach to small swarms with fixed obstacle configurations.

Limitations of existing paradigms and position of this work. A critical gap emerges across these approaches: all rely on deterministic rules and predictable response patterns, collectively struggling with:

– systematic coverage gaps in non-convex geometries;
– high parameter sensitivity to environment-specific thresholds;
– scalability degradation as swarm size grows;
– local minima entrapment causing revisitation of scanned areas.

Prior work on multi-level swarm architectures [8] and swarm survivability [10] confirms these limitations even in architecturally sophisticated systems.

Our contribution addresses this gap by integrating deterministic chaos theory as the fundamental coordination mechanism. The ergodic properties of properly configured chaotic attractors generate dense coverage patterns that explore arbitrary territory geometries without systematic gaps, operating independently of obstacle geometry. Building on the Swarm Chemistry framework established in [11], we combine chaotic dynamics with separation, cohesion, alignment, and anti-jamming forces. The resulting distributed architecture provides inherent fault tolerance – analogous to the survivability approach of [10] – without centralized path recalculation overhead. Genetic algorithm-based parameter optimization replaces manual threshold selection with automated tuning.

Problem statement and technical challenges. We consider a heterogeneous UAV swarm tasked with covering a complex, obstacle-rich area. The mission is to reach a specified coverage level in minimal time, subject to constraints on collision avoidance, obstacle clearance and per-drone energy consumption.

The central difficulty is a mismatch: classical chaotic algorithms behave uniformly, whereas real-world territories differ widely in geometry. While chaotic trajectories provide dense coverage, a single fixed parameter configuration cannot be optimal for all landscape types [16], [17]. Open spaces, deep concavities, corridor-like structures, and obstacle-dense zones each require different coordination regimes. Without adaptation to the territory profile, the algorithm either under-explores complex regions or wastes resources on redundant traversal in simpler zones.

This observation motivates the research question addressed in the present work: "*can a closed-loop mapping from measurable territory geometry metrics to chaotic motion parameters produce statistically superior coverage outcomes across a diverse set of operational scenarios, compared to a static optimally-tuned parameter set?* ".

Territory complexity as an algorithmic input. Classical approaches to UAV path planning treat the operational area as a known but passive entity: it imposes geometric constraints, yet tells the movement strategy nothing beyond which cells are free and which are blocked. We regard this as a fundamental architectural limitation. Five measurable geometric properties of Ω can inform the choice of chaotic parameters.

1. Concavity index. $\kappa \in [0,1]$ quantifies the fraction of the convex hull area $|\mathcal{H}(\Omega)|$ not covered by Ω:

$$\kappa = 1 - \frac{|\Omega|}{|\mathcal{H}(\Omega)|}. \tag{1}$$

High concavity ($\kappa > 0.3$) implies re-entrant pockets that chaotic trajectories with low cohesion will systematically miss. Parameter adaptation must increase unscanned-area bias and swarm cohesion in response.

2. Obstacle density. $\rho_o \in [0,1]$ is the fraction of $|\Omega|$ occupied by impassable obstacles:

$$\rho_o = \frac{\sum_{k=1}^{m} \pi r_k^2}{|\Omega|}. \tag{2}$$

Dense obstacle fields ($\rho_o > 0.1$) produce local minima for chaotic trajectories; the anti-jamming detection zone must enlarge and trigger more frequently.

3. Narrow corridor factor. $\gamma \in [0,1]$ estimates passage narrowness via progressive polygon erosion: the minimum erosion radius r^* at which Ω becomes topologically empty, normalized by the characteristic half-width $\bar{w} = |\Omega|/|\partial\Omega|$. Values $\gamma < 0.5$ signal that swarm spread must contract to prevent agents from mutually blocking passage entrances.

4. Point density. $\delta = |\Omega|/|\mathcal{B}(\Omega)|$, where $\mathcal{B}(\Omega)$ is the bounding box of Ω, measures how much usable area the swarm can access relative to the navigation envelope. Elongated or perforated geometries ($\delta < 0.7$) call for finer angular sampling so that thin protrusions are reached at all.

5. Dynamic coverage metrics. These include coverage progress $\varphi(t) \in [0,1]$, redundancy ratio $\rho_r(t)$, unscanned cluster count $C_u(t)$, and boundary pressure $\beta(t)$, which together form the dynamic layer of the territory profile and change continuously during the mission. Efficient progress is indicated by low ρ_r and monotonically decreasing C_u; deviations signal behavioral pathologies that require parameter correction.

Technical challenges. Territory-aware adaptive chaotic control raises several challenges.

1. Lack of analytical mapping. No direct formula links chaotic parameters to coverage quality, so adaptation must rely on empirically derived rules – and those rules must not work against one another.

2. Temporal stability. Abrupt parameter changes can destabilize the swarm, so adaptation must move parameters smoothly and keep them from drifting.

3. Computational cost. Calculating territory metrics in real time is resource-intensive; the system must balance metric update frequency with performance constraints.

4. Rule conflicts. Simultaneous activation of multiple adaptation rules can push parameters beyond safe limits, requiring bounded aggregation to maintain stability.

5. Heterogeneous swarm generalization. Adaptation must remain robust across drones with different speeds, battery profiles, and scan widths, ensuring effective coordination for mixed fleets.

Methodology. During the development of the adaptive chaotic algorithm, nine key motion parameters were identified and are hereafter denoted by compact mathematical symbols: b (preference for unscanned areas), ξ (swarm cohesion strength), τ (swarm stuck threshold), z (anti-jamming zone size), Δt_c (anti-jamming check interval), n_d (direction sample count), $s_{\max}$ (maximum swarm spread), t_r (redirect cooldown), T_v (area vector update interval), $\psi_{\max}$ (maximum turn rate). These parameters are combined into the vector $\theta = (b, \xi, \tau, z, \Delta t_c, n_d, s_{\max}, t_r, T_v, \psi_{\max})$ and are used throughout the subsequent formulations, tables, and adaptation rules.

The proposed method consists of three tightly coupled layers:

– chaotic area movement engine with swarm chemistry forces;

– territory analyzer that derives a geometric and dynamic profile of the operational area;

– closed-loop adaptive parameter controller that maps the territory profile to concrete algorithm parameters via a rule-based policy with smooth interpolation.

Together these layers form a feedback-controlled chaotic swarm, visualized in Fig. 1.

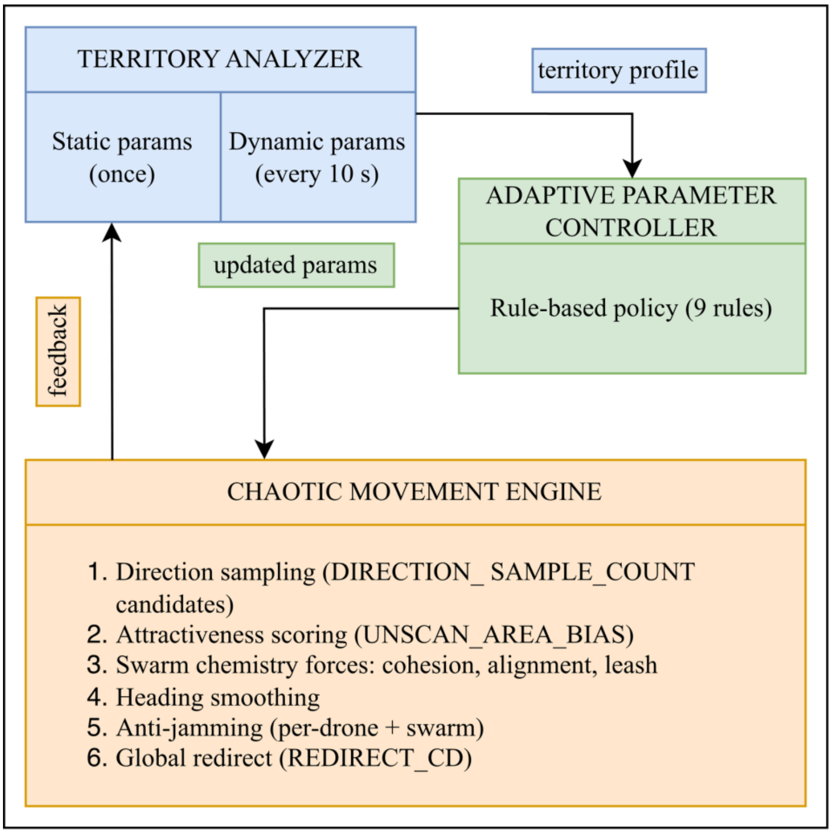

Fig. 1. **Architecture of the adaptive chaotic swarm control loop**

Source: **compiled by the authors**

Chaotic area movement engine. Each agent d_i executes the following motion pipeline every tick. A shared global area vector $v = (\cos\varphi, \sin\varphi)$ provides a soft preferred heading that is periodically re-oriented toward the centroid of the largest cluster of unscanned cells, found via DBSCAN every T_v second.

Direction selection samples n_d candidate headings and scores each via an attractiveness function that heavily penalizes already-scanned cells:

$$a(k) = w_{\text{unscan}}(k) \cdot b^{\mathbf{1}[\text{unscan}(k)]} + w_{\text{head}} \cdot \cos(\theta_k - \psi_i), \quad (3)$$

where b is the unscanned-area bias multiplier, ψ_i is the current heading of agent d_i, and $w_{\text{head}} = 0.15$ softly penalizes large heading changes.

Four swarm chemistry forces act additively on the desired heading after direction selection: separation – repulsion from neighbors within `SAFE_DISTANCE`; cohesion – attraction toward the local neighbourhood centroid scaled by ξ; alignment – tendency to match neighbour headings, weighted by $w_{\text{align}} = 0.35$; centroid leash – exponential-moving-average pull toward the swarm-wide centroid when separation exceeds $s_{\max}$.

Heading updates are smoothed to prevent oscillation: the desired angle $\hat{\psi}$ passes through an EMA with $\alpha_s = 0.25$, and the resulting turn is clamped to $\pm\psi_{\max}$ per tick.

Anti-jamming operates at two levels. Individually, a drone is judged stuck once it has visited fewer than z unique grid cells over the last `ANTI_JAMMING_STUCK_THRESHOLD` check intervals (each of length Δt_c seconds), and triggers a targeted escape maneuver to a randomly sampled unscanned destination. At the swarm level, if the fraction of agents currently located in already-scanned cells exceeds τ for `SWARM_STUCK_CONSECUTIVE` = 4 consecutive checks, a single global redirect target is chosen from unscanned space and broadcast to all agents; the redirect is suppressed for t_r seconds afterward to prevent thrashing.

Table 1 lists all adaptable parameters at their baseline values; Table 2 lists the per-parameter safe operating bounds enforced during adaptation.

Table 1. **Baseline values of adaptable algorithm parameters**

Symbol	Baseline	Role
b	2.0	Unscanned-area bias multiplier
ξ	0.9	Swarm cohesion strength
τ	0.35	Swarm stuck threshold
z	3	Anti-jamming zone size
Δt_c	3.0 s	Anti-jamming check interval
n_d	10	Direction sample count
$s_{\max}$	30.0	Maximum swarm spread
t_r	5.0 s	Redirect cooldown
T_v	1.5 s	Area vector update interval
$\psi_{\max}$	10.0°	Maximum turn rate

Source: **compiled by the authors**

Table 2. **Safe operating bounds for adaptive parameter clamping**

Symbol	Min	Max
b	0.5	5.0
ξ	0.3	2.0
τ	0.10	0.60
z	1	8
Δt_c	0.5 s	5.0 s
n_d	5	20
$s_{\max}$	10	80
t_r	2.5 s	15.0 s
T_v	0.5 s	5.0 s
$\psi_{\max}$	5.0°	30.0°

Source: **compiled by the authors**

Territory analyzer. The TerritoryAnalyzer module partitions the territory profile into two layers with different computational costs.

1. Static layer (computed once at mission start from polygon Ω): concavity index κ (1), obstacle density ρ_o (2), narrow corridor factor γ, point density δ, and isoperimetric ratio $Q = 4\pi|\Omega|/|\partial\Omega|^2$.

2. Dynamic layer (recomputed every Δt): fast metrics – coverage progress $\varphi(t)$ and redundancy ratio $\rho_r(t)$ – are recomputed from the coverage grid every tick in $O(1)$ using `numpy`; slow metrics – unscanned cluster count $C_u(t)$ via DBSCAN and boundary pressure $\beta(t)$ – are cached with $\Delta t_{\text{slow}} = 10$ s to avoid blocking the control loop, as this interval is chosen to minimize computational load from heavy metrics. The merged profile $\mathrm{s}(t) = \{\kappa, \rho_o, \gamma, \delta, \varphi, \rho_r, C_u, \beta\}$ is passed to the Adaptive Controller every $T_{\text{adapt}} = 5$ s, which is selected to ensure rapid adaptation of the controller to changing conditions.

Adaptive parameter controller. The controller implements a rule-based policy $f\colon \mathrm{s}(t) \mapsto \theta^*$ that computes a target parameter vector relative to the fixed baseline θ_0 (Table 1). Nine rules fire independently; their additive contributions are subject to a bounded composition constraint that prevents any parameter subset from exceeding its safe operating range (Table 2). The target vector is then refined to ensure consistency and prevent conflicting parameter interactions.

Table 3 summarizes the nine rules, the territory conditions that activate them.

Table 3. **Adaptive parameter rules**

№	Condition	Adjustment (Δ from baseline)
1	$\kappa > 0.3$	$\uparrow b, \uparrow \xi, \downarrow \tau$ *
2	$\rho_o > 0.1$	$\uparrow z, \downarrow \Delta t_c, \uparrow n_d$
3	$\gamma < 0.5$	$\downarrow \xi, \downarrow s_{\max}$
4	$\varphi > 0.7$	$\downarrow T_v, \uparrow b$
5	$C_u > 3$	$\downarrow t_r$
6	$\rho_r > 0.25$	$\uparrow b, \downarrow t_r, \downarrow T_v$
7	$\beta > 0.6$	$\uparrow s_{\max}, \downarrow \xi, \downarrow t_r$
8	$\delta < 0.7$	$\uparrow \psi_{\max}, \uparrow n_d$
9	$\varphi > 0.5$	$\uparrow \tau$
* Rule 1 adjusts τ only when $\varphi \le 0.7$ (Rule 9 takes precedence).		

Source: **compiled by the authors**

Rules 5, 6, and 7 all reduce t_r. To prevent their simultaneous firing from collapsing the cooldown to its minimum bound and causing continuous global redirects, a composition cap enforces:

$$t_r^* \ge t_{r,0} - 3.0 \text{ s} \tag{4}$$

The target θ^* is never applied immediately. Instead, the controller uses per-parameter linear interpolation to guarantee smooth parameter trajectories, preventing transient instabilities caused by abrupt changes in ξ or t_r. The interpolation rate $\alpha = 0.35$ was selected to yield convergence within three to four adaptation cycles while remaining responsive to rapid coverage progress changes.

Genetic algorithm for offline baseline optimization. Prior to deployment, drone recipes (scan width w_s, current speed v, max speed $v_{\max}$, and count) are optimized via a genetic algorithm (GA) with population size $P = 10$ and $G = 20$ generations.

The fitness function minimizes a weighted sum:

$$\mathcal{F}(\mathbf{r}) = \textstyle\sum_i \left[\left(100 - w_{s,i}\right) + 0.01\, w_{s,i}^2 + 0.02\, v_i^2 + \lambda\left(E_{0,i} - E_i\right)\right], \tag{5}$$

where λ is the energy penalty factor. Crossover is uniform at the recipe level; mutation perturbs $w_s \in [30,50]$ and $v \in [v_{\min}, v_{\max}]$ each with probability 0.3. Tournament selection with size 2 is applied over all generations. The GA optimizes swarm recipe composition offline; the resulting recipe is fixed at mission start, while the adaptive controller handles online parameter tuning during flight.

Experimental setup and results. All experiments were conducted in a discrete-grid simulation environment. The configuration below was deliberately held fixed across both modes so that the paired comparison isolates the effect of adaptation rather than of scenario variation:

– Map: 53×40 cells (area = 2120 cells), 3 circular obstacles;
– Swarm: 3 Matrice-class UAVs (DRONE-1, DRONE-2, DRONE-3);
– Initial energy: 593 Wh per agent (total 1779 Wh);
– Mission time limit: 60 s (all runs terminated by time limit);
– Trials: $N = 50$ per mode (adaptive / non-adaptive);
– Obstacle density range: 0.032–0.299 (mean ≈ 0.160).

Two modes were compared under identical conditions: adaptive – online closed-loop parameter adaptation via the territory analyzer; non-adaptive – fixed baseline parameters (Table 1) with no runtime adjustment. One run per mode yielded zero coverage due to initialization failure and was treated as an anomaly (2% failure rate, identical in both modes). Statistical significance was assessed with the two-sided Mann-Whitney U test ($\alpha = 0.05$, $U_{\text{crit}} \approx 966$).

Scale of the test bench. Swarm size and territory footprint are controlled variables here rather than claimed operating limits: both were fixed so that the paired comparison isolates the effect of adaptation, the present territory (2120 cells) already exceeding the 34×23-cell grid of [16] by a factor of 2.7. The proposed contribution is by construction invariant to swarm size: the territory analyzer is bounded by the grid and not by the swarm (static profile computed once, fast metrics recomputed per tick, slow metrics cached at Δt_{slow}), and the controller is $O(1)$ in both quantities, since the nine rules act on the aggregated profile $s(t)$ and θ^* is broadcast swarm-wide. Enlarging the swarm therefore leaves the adaptation layer unchanged and affects only the underlying movement engine, whose $O(n^2)$ pairwise neighbourhood query spatial indexing reduces to $O(n \log n)$, and which, as established in [16], remains real-time up to n ≈ 30-40 agents unindexed and 50-100 indexed. A larger footprint at a fixed horizon lowers the attainable coverage fraction proportionally and requires the horizon to be rescaled, whereas the adaptive advantage should widen rather than narrow, since larger areas sustain higher C_u and β – the conditions activating Rules 5 and 7. Empirical validation at larger swarm sizes – three agents were used here and five in [11] – and at an order-of-magnitude larger footprint is a stated limitation of the present study and the subject of ongoing work.

Primary results. Table 4 presents the core comparative metrics across all $N = 50$ trials per mode.

Table 4. **Primary comparative metrics ($N = 50$ trials per mode)**

Metric	Adaptive	Non-Adapt.	Δ	p-val
Coverage (%) mean	38.63	33.59	+5.04 pp	<0.05
Coverage (%) median	39.53	34.37	+5.16 pp	–
Coverage CV%	14.43	17.87	−3.44 pp	–
Region coverage (%)	55.96	48.66	+15.0 %	<0.05
Distance (m) mean	24,434	18,892	+5,542 m	<0.05
Distance CV%	13.80	9.76	–	–
Energy (Wh) mean	586.0	453.2	+132.8 Wh	<0.05
Redund. scan (%) mean	33.82	32.15	+1.67 pp	<0.05

Source: **compiled by the authors**

The adaptive mode achieves +15.0 % higher mean territory coverage (38.63% vs. 33.59 %) with a statistically significant difference ($U_{\min} = 0.0 \ll U_{\text{crit}}$). The improvement in region-level coverage is equally pronounced: 55.96 % vs. 48.66 %. Critically, the adaptive mode also yields a lower coefficient of variation (CV = 14.4 % vs. 17.9 %), confirming that adaptation increases not only mean performance but also run-to-run consistency.

The 29.3 % increase in total distance traveled (24434m vs. 18892m) constitutes the mechanistic explanation for the coverage gain: the adaptive controller redirects agents toward uncovered clusters (Rules 4-7 in Table 3), preventing trajectory stagnation and extending effective exploration path length within the fixed time budget.

Coverage distribution. Table 5 shows how trials distribute across coverage bins, highlighting the rightward shift produced by adaptation.

Table 5. **Coverage distribution across 50 trials per mode**

Coverage range	Adaptive	Non-Adaptive
0-10 %	1	1
10-20 %	1	1
20-30 %	1	7
30-40 %	27	37
40-50 %	20	4

Source: **compiled by the authors**

Twenty adaptive trials (40 %) achieve the 40-50 % coverage bin, compared to only 4 non-adaptive trials (8 %). The non-adaptive mode concentrates 74 % of its results in the 30-40 % bin, reflecting the ceiling imposed by fixed parameter stagnation.

Energy and efficiency trade-offs. The adaptive mode consumes 29.3 % more energy on average (586.0 Wh vs. 453.2 Wh), proportional to the increase in distance traveled. However, in emergency response and search-and-rescue scenarios – where maximizing absolute area coverage within a fixed time window is the primary objective – this trade-off is operationally acceptable: the available energy budget is consumed productively in active exploration rather than idle hovering or redundant revisitation. The redundant scan fraction increases only marginally (+1.67 pp), confirming that the additional flight path is directed primarily toward new cells.

Pairwise comparison and outlier analysis. Run-by-run comparison shows the adaptive mode winning in 33 of 50 trials (66 %) with no ties. Table 6 lists runs with $|\Delta\text{cov}| > 10$ %.

Table 6. **Runs with large coverage deviation ($|\Delta| > 10\%$)**

Run	Adap. (%)	Non-Ad. (%)	Δ	Winner
#49	42.85	0.00	+42.85	Adaptive
#13	37.20	1.37	+35.83	Adaptive
#40	0.00	34.06	−34.06	Non-Adapt.
#10	16.68	39.58	−22.89	Non-Adapt.
#5	26.86	42.97	−16.11	Non-Adapt.
#41	47.58	32.41	+15.17	Adaptive
#0	48.12	36.65	+11.47	Adaptive

Source: **compiled by the authors**

Runs #49 and #13 represent cases of near-complete non-adaptive failure (initialization anomaly and immediate stagnation, respectively) recovered by the adaptive controller. The three non-adaptive wins (#40, #10, #5) correspond to low-concavity open-field configurations where baseline parameters are already near-optimal and adaptation overhead introduces marginal trajectory perturbations.

Conclusions. This paper presented a territory-aware adaptive chaotic movement algorithm for autonomous area coverage by UAV swarms in emergency response scenarios. Its core contribution is a closed-loop architecture that continuously maps measurable geometric and dynamic properties of the operational territory – concavity index κ, obstacle density ρ_o, narrow corridor factor γ, point density δ, and real-time coverage progress metrics – to nine swarm chemistry motion parameters $\theta = (b, \xi, \tau, z, \Delta t_c, n_d, s_{\max}, t_r, T_v, \psi_{\max})$ via a rule-based adaptive controller with linear interpolation smoothing.

Experimental validation across 50 simulation trials per mode yielded three principal findings. First, the adaptive mode achieved statistically significant improvements in mean territory coverage ($+5.04$ pp, $+15.0\%$ relative, $p < 0.001$), region-level coverage, total distance traveled, and energy consumption ($p < 0.001$ for all these metrics), confirming that territory-driven parameter adaptation provides substantially better results on the main efficiency criteria. Second, there is a marked increase in stability: the coefficient of variation decreases from 17.87 % to 14.43 %, indicating reduced sensitivity to random factors and initialization. Third, differences in redundant scan and obstacle density do not reach statistical significance ($p > 0.05$), indicating that these aspects of the algorithm remain stable when switching to adaptive mode.

This underscores the specificity and targeted nature of the improvements achieved through adaptive control. In practical terms, the adaptive algorithm delivers robust gains in the most operationally relevant metrics: coverage, region-level coverage, distance, and energy while maintaining stability in secondary characteristics such as redundant scanning and sensitivity to obstacle density. Thus, the adaptation mechanism enhances mission-critical performance without introducing instability or unintended trade-offs in other aspects of swarm behavior.

The mechanistic basis of the gain is the active redirection of agents toward uncovered spatial clusters via reduction in t_r and T_v (Rules 4-7 in Table 3), which increases total path length by 29.3% and energy consumption proportionally. The marginal growth in redundant scanning ($+1.67$ pp) confirms that the additional flight effort translates primarily into new-cell coverage rather than revisitation – a decisive criterion in time-critical missions. Where baseline parameters are already near-optimal – that is, in low-concavity open-field configurations – adaptation adds small trajectory perturbations without a compensating gain, which accounts for the 17 of 50 paired trials won by the non-adaptive mode. This marks out the operating regime in which adaptation yields a net benefit.

Three extensions follow naturally from this work. First, the nine rule-based adjustments were derived from domain analysis and validated empirically; replacing this hand-crafted policy with a learned mapping – for instance, multi-objective Bayesian optimization over recorded mission trajectories – could improve parameter quality further while reducing design effort. Second, the current formulation treats territory analysis and parameter adaptation as swarm-level operations with shared parameter broadcast; extending to per-agent heterogeneous adaptation would leverage the diversity of battery profiles and sensor capabilities within the drone family. Third, the simulation abstracts away the physical disturbances of real flight – communication latency, GNSS positioning error and wind – whose compensation the architecture already localizes. Latency is tolerated by construction: s(t) reaches the controller only every T_{adapt} = 5 s and θ^* is approached over three to four interpolation cycles, so link delays of tens to hundreds of milliseconds shift the parameter trajectory rather than destabilize it, the single broadcast redirect being the latency-critical path and t_r its natural retransmission window. Positioning error is absorbed by inflating `SAFE_DISTANCE` and the anti-jamming zone z – whose upper bound in Table 2 already reserves headroom – by the 3σ radius of the navigation solution, and by marking cells scanned from measured rather than commanded positions, so that uncertainty yields conservative re-scanning rather than undetected gaps. Wind enters as a bias between commanded heading and observed ground track, is estimated from that residual over the EMA window and compensated as a "crab angle", with $\psi_{\max}$ and a_s bounding the control effort. Software-in-the-loop validation with a flight-dynamics model, followed by field trials, is the immediate next step.

The results establish terrain-aware chaotic adaptation as a principled, statistically validated, and operationally interpretable strategy for autonomous UAV swarm area scanning – a foundational capability for higher-level emergency response mission execution.

Conflict of interests: The authors declare that they have no conflict of interests, in particular financial, personal, copyright or any of a different nature, which could have influenced the research, as well as the results published in this article

Financing: Research was carried out without financial support

Accessibility data: All data available in digital or graphic form in the main text of the manuscript

Using artificial intelligence tools: The authors confirm that they did not use instrumental artificial intelligence tools for writing this work.

REFERENCES

1. Silvagni, M., Tonoli, A., Zenerino, E. & Chiaberge, M. "Multipurpose UAV for search and rescue operations in mountain avalanche events". *Geomatics, Natural Hazards and Risk*. 2017; 8 (1): 18–33. DOI: https://doi.org/10.1080/19475705.2016.1238852.

2. Huang, H. & Savkin, A. V. "Path planning for a solar-powered UAV inspecting mountain sites for safety and rescue". *Energies*. 2021; 14 (7): 1968. DOI: https://doi.org/10.3390/en14071968.

3. Abdullahi, A., Chindo, A. M., Bisola, O. A., Danladi, A., Fakunle, S. O., Anthony, O., Muyideen, A. A., Idowu, A., Adeola, O. S. & Ashem, N. M. "A study of the communication system of an unmanned aerial vehicles (UAVs)". *International Journal of Trend in Scientific Research and Development*. 2026; 10 (1): 721–728. – Available from: www.ijtsrd.com/papers/ijtsrd100120.pdf – [Accessed: 16.06.2026].

4. Campion, M. & Ranganathan, P. "UAV swarm communication and control architectures: a review". *Drone Systems and Applications*. 2019; 7 (2): 93–106. DOI: https://doi.org/10.1139/juvs-2018-0009.

5. Alakbarov, Z. & Bekirova, L. "UAV swarm systems". *PAHTEI-Proceedings of Azerbaijan High Technical Educational Institutions*. 2023; 34 (4): 274–284. DOI: https://doi.org/10.36962/PAHTEI34112023-274.

6. Javed, S., Hassan, A., Ahmad, R. & Ahmed, W. "State-of-the-art and future research challenges in UAV swarms". *IEEE Internet of Things Journal*. 2024; 11 (11): 19023–19045. DOI: https://doi.org/10.1109/JIOT.2024.3364230.

7. Li, J., Yue, Q., Huang, Z., Xie, X. & Yang, Q. "Vulnerability analysis of UAV swarm network with emergency tasks". *Electronics*. 2024; 13 (11): 2005. DOI: https://doi.org/10.3390/electronics13112005.

8. Tsariuk, A. O. & Malakhov, E. V. "The multilayer distributed intelligence system model for emergency area scanning". *Herald of Advanced Information Technology*. 2021; 4 (3): 268–277. DOI: https://doi.org/10.15276/hait.03.2021.6.

9. Egglestone, P., Ansell, D. & Cook, C. "UAVs in crowd tagged mountain rescue". *Proceedings of MindTrek 2013*. Tampere, Finland. 2013. p. 1–5. – Available from: https://www.academia.edu/4505249/UAVs_in_crowd_tagged_mountain_rescue [Accessed: 02.08.2025].

10. Samburskyi, V. & Malakhov, E. "Improving the survivability of a reconnaissance UAV swarm based on cellular automata". *Proceedings of the 2024 International Conference on Unmanned Aerial Systems*. 2024. p. 310–315. DOI: https://doi.org/10.1145/3674558.3674603.

11. Kozlov, M. S. & Shvets, Y. O. "Heterogeneous swarm complex multilevel reconfiguration based on Swarm Chemistry". *Applied Aspects of Information Technology*. 2025; 8 (2): 147–161. DOI: https://doi.org/10.15276/aait.08.2025.10.

12. Kozlov, M. S. & Malakhov, E. V. "A complex model of human recognition in emergencies by a multi-level drone system". *2024 International Symposium ELMAR*. Zadar, Croatia. 2024. p. 317–320. https://www.scopus.com/pages/publications/85207193007. DOI: https://doi.org/10.1109/ELMAR62909.2024.10694255.

13. Liu, X. "Research on improved A* path planning of UAV for dynamic obstacle avoidance". *Journal of Physics: Conference Series*. 2025; 3169: 012058. DOI: https://doi.org/10.1088/1742-6596/3169/1/012058.

14. Hu, Y., Wu, Y. & Chen, W. "Multi-UAV swarm obstacle avoidance based on potential field optimization". *Journal of Intelligent Systems*. 2024; 13: 1–20. DOI: https://doi.org/10.48550/arXiv.2511.16911.

15. Keribayeva, T., Koshekov, K., Alibekkyzy, K., Koshekov, A. & Ivanova, M. "Modeling obstacle avoidance strategies in UAV groups". *Naukovyi Visnyk Natsionalnoho Hirnychoho Universytetu*. 2025; 2: 206–220. DOI: https://doi.org/10.33271/nvngu/2025-2/206.

16. Kozlov, M. S., Malakhov, E. V. & Shvets, Y. O. "Comparative analysis of chaotic and deterministic methods to territory coverage by drone swarms". *Herald of Advanced Information Technology*. 2025; 8 (4): 447–463. https://www.scopus.com/pages/publications/105026617701. DOI: https://doi.org/10.15276/hait.08.2025.28.

17. Kozlov, M. S., Malakhov, E. V., Samikannu, R., Shvets, Y. O. "AI-Assisted optimization of multi-agent system parameters: A model of iterative hyperparameter tuning in swarm intelligence algorithms". *Applied Aspects of Information Technology*. 2026; 9 (3), 310–325. DOI: https://doi.org/10.15276/aait.09.2026.21.

Received 03.08.2026
Received after revision 29.08.2026
Accepted 04.09.2026

DOI: https://doi.org/10.15276/ict.03.2026.38
УДК 681.5:004.89

Динамічна адаптація параметрів хаотичного руху безпілотних літальних апаратів на основі аналізу складності місцевості

Козлов Микита Сергійович[1)]
ORCID: https://orcid.org/0009-0007-0071-7748; nikita.kozlov@stud.onu.edu.ua
Малахов Євген Валерійович[1)]
ORCID: https://orcid.org/0000-0002-9314-6062; eugene.malakhov@onu.edu.ua. Scopus Author ID: 56905389000
[1)] Одеський національний університет імені І. І. Мечникова, вул. Дворянська, 2. Одеса, 65082, Україна

АНОТАЦІЯ

Автономні рої безпілотних літальних апаратів дедалі ширше застосовуються в операціях реагування на надзвичайні ситуації та в пошуково-рятувальних роботах. Проте наявні алгоритми планування траєкторій на основі маршрутних точок демонструють систематичні прогалини в покритті неопуклих територій і не здатні адаптуватися до змінних умов середовища під час виконання місії. Тому в роботі запропоновано адаптивний алгоритм хаотичного руху рою безпілотних літальних апаратів, який ураховує характеристики місцевості та динамічно коригує параметри руху на основі вимірюваних геометричних властивостей операційної зони, зокрема індексу увігнутості, щільності перешкод, коефіцієнта вузьких коридорів і показників прогресу покриття в реальному часі. Адаптивний контролер із замкненим контуром зіставляє профіль місцевості з дев'ятьма параметрами рою за допомогою правил на основі лінійної інтерполяції зі згладжуванням. Експериментальне оцінювання за результатами п'ятдесяти імітаційних випробувань показує, що адаптивний режим забезпечує на п'ятнадцять відсотків вище середнє покриття території та зменшує розкид між запусками на дев'ятнадцять відсотків порівняно з базовим варіантом із фіксованими параметрами. Статистичний аналіз за U-критерієм Манна–Уітні підтверджує, що поліпшення покриття на рівні регіонів, загальної пройденої відстані та споживання енергії є високозначущими, тоді як відмінності в надлишковому скануванні та щільності перешкод – ні. Ці результати підкреслюють, що основні експлуатаційні переваги адаптивного алгоритму є надійними та відтворюваними, а другорядні показники залишаються стабільними в усіх режимах. Отримані результати підтверджують, що хаотична адаптація з урахуванням рельєфу місцевості є принциповою та практично придатною стратегією автономного сканування території.

Ключові слова: Інформаційні технології; ройовий інтелект; хаотичний алгоритм; багатоагентні системи; оптимізація сканування; оптимізація траєкторії рою; аналіз зони сканування

ABOUT THE AUTHORS

Mykyta S. Kozlov - PhD student of Computer Science. Odesa I. I. Mechnikov National University, Odesa, 65082, Ukraine. Senior Software Development Engineer at SPD-Tech, Cherkasy, Ukraine
ORCID: https://orcid.org/0000-0001-8130-9613; nikita.kozlov@stud.onu.edu.ua
***Research field*:** Computer vision, swarm technology, artificial intelligence

Козлов Микита Сергійович - аспірант Комп'ютерних наук. Одеський національний університет імені І.І. Мечникова, Одеса, 65082, Україна. Senior Software Development Engineer (Back-End), SPD-Tech, Черкаси, Україна
Галузь досліджень: комп'ютерний зір, штучний інтелект

Eugene V. Malakhov - Doctor of Engineering Science, Professor, Head of Department of Mathematical Support of Computer Systems. Odesa I. I. Mechnikov National University, Odesa, 65082, Ukraine
ORCID: https://orcid.org/0000-0002-9314-6062; eugene.malakhov@onu.edu.ua. Scopus Author ID: 56905389000
Research field: Databases theory, Metamodeling, Data Mining and other data structuring methods, Data Processing methods, Artificial Intelligence and Machine Learning

Малахов Євгеній Валерійович – доктор технічних наук, професор, завідувач кафедри Математичного забезпечення комп'ютерних систем. Одеський національний університет імені І.І. Мечникова, Одеса, 65082, Україна

Галузь досліджень: Теорія баз даних, метамоделювання, аналіз даних та інші методи структурування даних, методи обробки даних, штучний інтелект та машинне навчання